Oxidation of Magnetite Nanoparticles

Abstract:

The oxidation of magnetite to maghemite in aqueous solution has been studied using spectroscopy in the near IR. As the reaction progresses absorbance in the near IR region decreases proportionately. This reaction has been studied at various temperatures from 0°C to 80°C. Consistent with previous literature reports, a diffusion model best fits the observed rate of oxidation. This model predicts that the iron diffuses to the surface and is then oxidized. In this way, the concentration gradient necessary for diffusion is formed. The temperature dependence of the corresponding diffusion constant is described by an Arrhenius type equation with energy of activation of approximately 21.0 kcal/mole, which agrees well with literature reports in bulk at higher temperatures (170°C to 190°C). There is some debate as to whether UV light can help to catalyze the oxidation process. We have studied this effect using a 100mW multi-line 351/363 nm argon laser. The effect at 0°C is equivalent to a 7°C increase in temperature, which is not insignificant. However, it is still not significant enough to say that it is a photochemical process.

Introduction:

Iron oxides such as magnetite (Fe_3O_4) and maghemite (γ-Fe_2O_3) are ubiquitous in nature. Both magnetite and maghemite have been used as naturally occurring magnets for many years making it extremely useful. Other applications range from collecting energy from the sun to cleaning up radionuclides in polluted water[1]. Magnetite and maghemite have also been found on the surface of Mars. The formation of certain types of magnetite nanocrystals on the surface of Mars has been attributed to a certain class of bacteria[2]. Despite being very common minerals, the reactions that iron oxides undergo in the presence of oxygen and water are still an area of much debate.

Because metal oxides tend to be crystalline substances, the reactions they undergo will either be topotactic or reconstructive. In topotactic reactions, the crystal structures of each particle remain intact throughout the reaction. In reconstructive reactions, the crystal structures disassociate, react and then recrystallize. The mechanism for the oxidation of magnetite to maghemite is actually quite complicated. Electron microscopy of bulk magnetite particles before and after oxidation supports a topotactic transformation[3], because no change in size or shape is observed for the same particles before and after oxidation. Further supporting a topotactic transformation, the size distribution of particles in aqueous solution does not change significantly during the oxidation process as verified by TEM. For topotactic reactions, diffusion of one or more components must occur if the nanoparticle completely oxidizes. In the case of magnetite, the iron cations have a radius roughly half that of the oxygen anions. Because of this, the diffusion coefficient of oxygen in magnetite will be small relative to the diffusion coefficient of iron in magnetite. Previous studies have shown that iron diffusion is enough to explain the kinetics of the oxidation of magnetite to maghemite.[4] Diffusion studies based on the diffusion of radioactive iron tracers in magnetite particles have been used at high temperatures and relatively low oxygen partial pressures. Experimental evidence correlates changes in the diffusion coefficients due to changes in oxygen partial pressures with reactions that involve the formation of vacancies in the crystal octahedral lattice[5]. The formation of these vacancies is important for diffusion[6] and oxidation as it electrically compensates for the conversion of Fe^{2+} to Fe^{3+}.

Synthesis:

Magnetite particles were made by the coprecipitation of 1eq. of $FeCl_2$ and 2eq. of $FeCl_3$ in basic solution. 324mg of $FeCl_3$ (2mmol) and 127mg of $FeCl_2$ (1mmol) were added to 10mL of de-ionized water in a three-neck flask. The solution is stirred for 15 minutes with nitrogen bubbling through the solution. 8mL of 1M TMAOH is added to another three-neck flask. Nitrogen is bubbled through this solution for 15 minutes. The iron solution is then slowly added to the TMAOH solution via syringe and stirred vigorously for 5 minutes. The nitrogen bubbling and stirring are turned off. A magnet is used to separate the magnetite from the solution. The solution is decanted off. Using the magnet and decanting off the solution each time, the magnetite is washed three times with de-ionized water. After this, the particles were re-dissolved in 8mL of 1M TMAOH. The particles can be stored by bubbling nitrogen into the solution for 30 minutes.

Characterization:

The size of the magnetite nanoparticles were determined to be 8.6 +/- 1.6 nm using TEM. The size of the corresponding oxidized maghemite nanoparticles were determined to be 8.7 +/- 1.2nm using TEM. To determine the extent to which the particles have oxidized, UV-Vis-Near IR absorption spectroscopy is used. Due to the charge transfer between Fe^{2+} and Fe^{3+}, magnetite has finite absorption into the near IR, as confirmed by Mie calculations. For maghemite, a semiconductor, absorption is expected to go to zero in the near IR. By monitoring the decrease in absorbance in the region, the extent of oxidation is determined at various times.

Kinetics:

Because the conversion of maghemite to magnetite is a topotactic reaction, this allows the kinetics to be accurately modeled without having to consider free Fe^{2+} and Fe^{3+} in solution. Oxygen (O^{2-}) has a radius roughly twice that of iron cations (Fe^{2+} and $Fe^{3}+$). Because O^{2-} is bigger than the iron cations, O^{2-} is not as mobile as the cations and the diffusion constant is several orders of magnitude less than that of the cations. A simplified model for the oxidation process will be considered in which only the iron diffuses to the surface where it is oxidized and oxygen is added. At relatively high oxygen concentrations, the oxidation at the surface is relatively high because the rate of oxidation at the surface is first order with respect to oxygen concentration. Under these conditions, the overall rate of oxidation is entirely determined by the rate of diffusion. At lower oxygen concentrations, the model should incorporate both the rate of oxidation at the surface and the rate of diffusion. The high oxygen concentration approximation will be used to analyze our initial oxidation studies, which were done in the open atmosphere. Diffusion in a sphere with no angular dependence can be represented as

$$\frac{\partial C}{\partial t} = D\left(\frac{\partial^2 C}{\partial r^2} + \frac{2}{r}\frac{\partial C}{\partial r}\right) \tag{1}$$

where D is the diffusion constant, C is the concentration of the iron species to be oxidized, r is the radial position, and t is the time. Substituting u = Cr into (1) we get

$$\frac{\partial u}{\partial t} = D\frac{\partial^2 u}{\partial r^2}. \tag{2}$$

As a first approximation, we will consider the case of fast oxidation at the surface, so that C = 0 at the surface of the sphere. Initially, the concentration throughout the sphere is C_0. Applying these boundary conditions and solving the diffusion equation, the concentration profile is

$$\frac{C_0 - C(r)}{C_0} = 1 + \frac{2a}{\pi r}\sum_{n=1}^{\infty}\frac{(-1)^n}{n}\sin\frac{n\pi r}{a}\exp\left(\frac{-Dn^2\pi^2 t}{a^2}\right) \tag{3}$$

where C_0 is the initial concentration of the iron species to be oxidized and a is the radius of the particle. Applying a mass balance and integrating appropriately, the conversion can be represented as

$$\frac{M_t}{M_\infty} = 1 - \frac{6}{\pi^2}\sum_{n=1}^{\infty}\frac{1}{n^2}\exp\left(\frac{-Dn^2\pi^2 t}{a^2}\right).$$

(4)

where M_t/M_∞ is assumed to be the extent of oxidation. For small t relative to a^2/D, this can be approximated as

$$\frac{M_t}{M_\infty} = \frac{6}{\pi^{1/2}}\left(\frac{Dt}{a^2}\right)^{1/2} - 3\frac{Dt}{a^2}.$$

(5)

Dividing both sides by t, we obtain

$$\left(\frac{M_t}{M_\infty}\right)\left(\frac{1}{t}\right) = \left(\frac{6}{\pi^{1/2}}\right)\left(\frac{D}{a^2}\right)^{1/2}\left(\frac{1}{t^{1/2}}\right) - 3\frac{D}{a^2}.$$

(6)

At lower oxygen concentrations, the rate of oxidation is no longer fast relative to the rate of diffusion. The boundary condition stating that C = 0 at the surface is no longer valid and must be replaced by an appropriate rate equation. At the surface the flux is equal to the rate of the reaction. Assuming a first order reaction with respect to both the iron and oxygen concentrations, we get

$$D\frac{\partial C(a)}{\partial r} = -k[O_2]C(a).$$

(7)

The concentration profile with this boundary condition is

$$\frac{C(r)}{C_0} = \frac{2La}{r}\sum_{n=1}^{\infty}\frac{\exp(-D\beta_n^2 t/a^2)}{\{\beta_n^2 + L(L-1)\}}\frac{\sin(\beta_n r/a)}{\sin(\beta_n)}$$

(8)

where β_ns are the roots of

$$\beta_n \cot \beta_n + L - 1 = 0 \tag{9}$$

and L = ak[O_2]/D. Applying a mass balance and integrating appropriately, the conversion can be represented as

$$\frac{M_t}{M_\infty} = 1 - \sum_{n=1}^{\infty} \frac{6L^2 \exp(-D\beta_n^2 t / a^2)}{\beta_n^2 \{\beta_n^2 + L(L-1)\}}. \tag{10}$$

Results:

Various samples of magnetite dissolved in aqueous solution were oxidized at room temperature, 50°C, 65°C, and 80°C. Aliquots of solution were taken out for analysis at various times depending on the reaction temperature. For samples oxidized at higher temperatures, aliquots were taken at relatively short intervals. For samples oxidized at room temperature, aliquots were taken over a period of several months. Immediately after the aliquots were taken, spectra were taken (see Figure 1). As the reaction progresses a decrease in absorbance is seen in the near IR region. Assuming that the decrease is linear with respect to conversion, extents of oxidations were calculated for various samples at different temperatures and times. For each temperature, the diffusion coefficients were determined using (6) (see Figures 2, 3, 4, and 5). These values are tabulated in table 1 as calculated using (6) from both the slope and the y-intercept. To determine the energy of activation and D_0 for the diffusion process, the average of the diffusion coefficient determined from the slope and the intercept is used (see Figure 6). The calculated energy of activation using the Arrhenius model is approximately 21.0 kcal/mole. D_0, the preexponential factor in the Arrhenius equation, was calculated to be approximately 7×10^{-5}

cm^2/sec. The energy of activation is in agreement with Sidhu, who did the oxidation under dry conditions. D_0 is within an order of magnitude with what is predicted by the theory of diffusion in crystalline solids, which estimates that D_0 equals $\lambda v/3$ where λ is the spacing between nearest iron cations neighbors in the lattice and v is the mean molecular velocity of the iron cations.

To investigate the effect that UV light has on the rate of conversion a multi-line 351/363 nm 100mW argon laser was used. A water bath (see Figure 7) was cooled used to cool a condenser (see Figure 8). A control was placed into the water bath with no light shining on it. Water circulates in the condenser. The laser shines through the side with the quartz cover slip and the condenser is filled with the solution. Aliquots were taken for analysis after 20, 70, 90, and 220 hours. The difference between these and the control corresponded to about a 7°C increase in temperature using the Arrhenius equation. This is significant, but we cannot discount the possibility that only a thermal effect is occurring.

Conclusion:

Future work will concentrate on the effects that lower oxygen partial pressures has on the kinetics of the reaction. By doing this, we would be able use (9) and (10) to analyze the kinetics of the oxidation at the surface. Current studies have prevented us from doing this, because diffusion entirely dominates the reaction.

Table 1

Temperature	24℃	50℃	65℃	80℃
D from Slope (cm^2/sec)	1.13795E-20	2.67E-19	9.69E-19	5.95E-18
D from Intercept (cm^2/sec)	1.50385E-20	2.43E-19	8.81E-19	5.61E-18

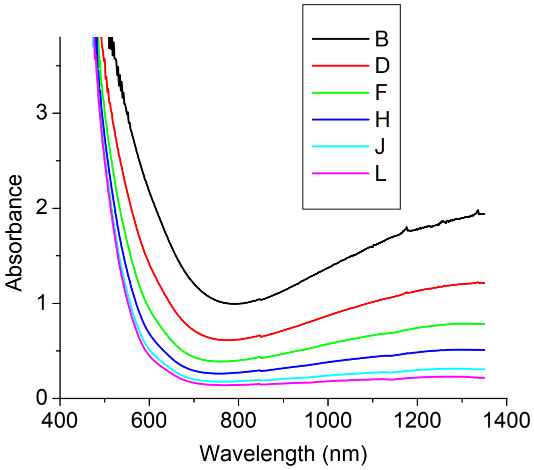

Figure 1 Spectra of aliquots taken at various times for reaction done at 80°C.

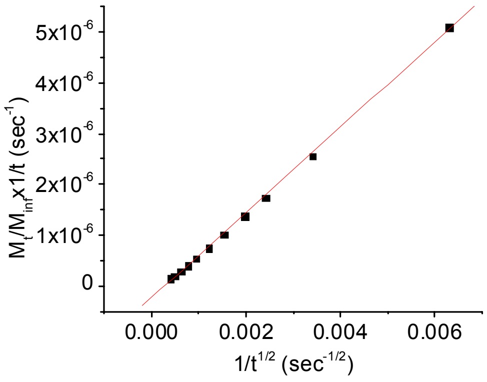

Figure 2 Plot M_t/M_∞ x 1/t vs. $1/t^{1/2}$ for reaction at room temperature

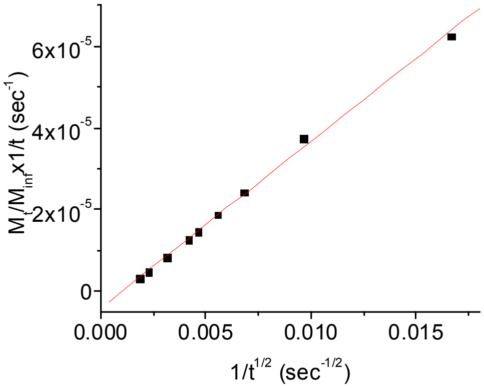

Figure 3 Plot M_t/M_∞ x 1/t vs. $1/t^{1/2}$ for reaction at 50°C

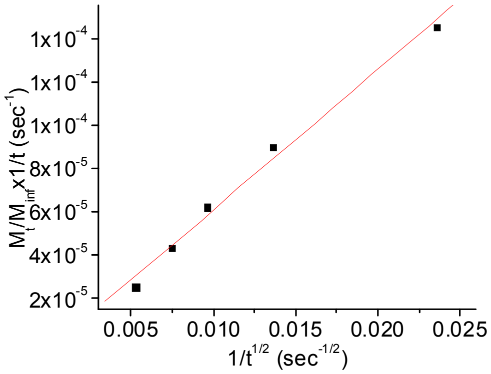

Figure 4 Plot M_t/M_∞ x 1/t vs. $1/t^{1/2}$ for reaction at 65°C

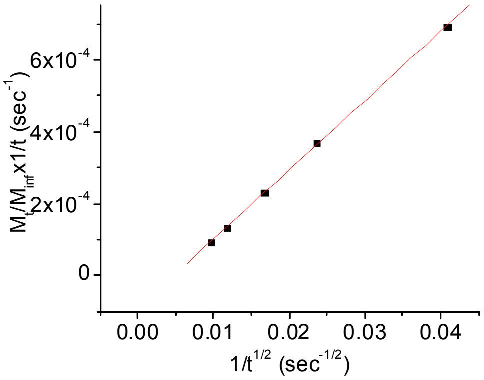

Figure 5 Plot M_t/M_∞ x 1/t vs. $1/t^{1/2}$ for reaction at 80°C

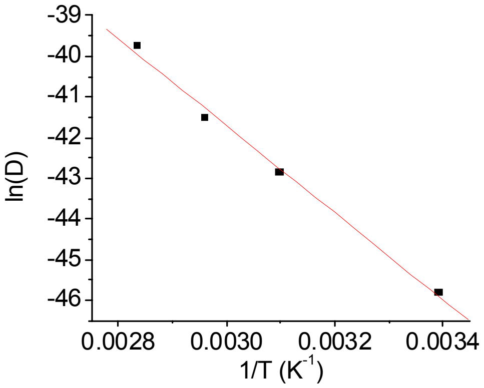

Figure 6 Arrhenius plot of diffusion coefficients

Figure 7

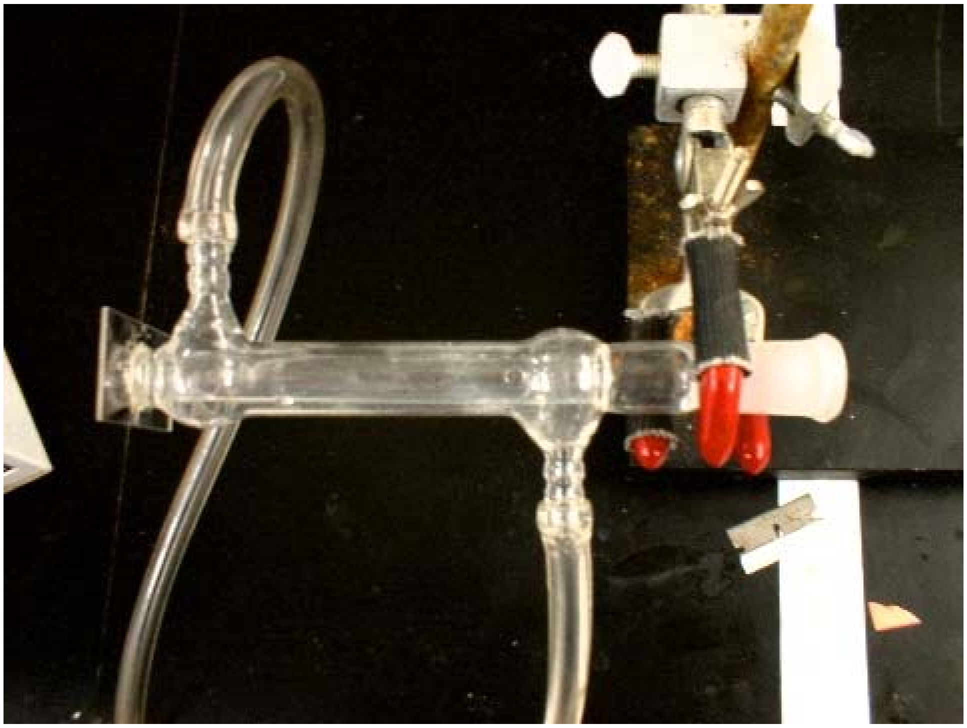

Figure 8

---

[1] Cornell, R.M., Schwertmann U., *The Iron Oxides*, VCH, 1996.

[2] Busek, P.R., Dunin-Borkowski R.E., Devouard, B., Frankel, R.B., McCartney, M.R., Midgley P.A., Posfai, M., and Weyland M., Proceedings of the National Academy of Science 98 (24): 13490-13495 2001.

[3] Sidhu P.S., Gilkes R.J., Posner A.M., Journal of Inorganic & Nuclear Chemistry 39 (11): 1953-1958 1977.

[4] Sidhu P.S., Gilkes R.J., Posner A.M., Journal of Inorganic & Nuclear Chemistry 39 (11): 1953-1958 1977.

[5] Peterson, N.L., Chen, W.K., Wolf, D., J. Phys. Chem. Solids 41: 709-719 1980.

[6] Jost, W., *Diffusion*. p. 135ff. Academic Press, New York, 1990.